THE JOURNAL OF PHYSICAL CHEMISTRY Letters

Letter

pubs.acs.org/JPCL

Photobasicity in Quinolines: Origin and Tunability via the Substituents' Hammett Parameters

Eric William Driscoll, Jonathan Ryan Hunt, and Jahan M Dawlaty*

University of Southern California, Los Angeles, California 90089, United States

Supporting Information

ABSTRACT: Coupling between electronic excitation and proton transfer is relevant to the kinetics of redox reactions, in particular those involved in solar-to-fuel light harvesting. A prime example of such coupling occurs in photoacids, where electronic excitation leads to proton release in the excited state. Here, we systematically study the inverse of this effect, photobasicity, in which a molecule becomes more basic in the excited state compared to the ground state. This endows the molecule with light induced proton removal capability which is anticipated to be of use in driving reactions where proton transfer is kinetically challenging. To investigate the origins and tunability of photobasicity, a set of 5-R-quinoline derivatives (R = {NH_2, CH_3O, H, Br, Cl, CN}) were selected and their changes in pK_a upon electronic excitation in aqueous solutions were determined. The Hammett parameters σ_p of these substituents, indicative of their electron withdrawing capability, span a range of −0.7 to +0.7. Using Förster cycle analysis, the acid dissociation equilibria in the ground and first excited state were determined. The ground state pK_a obeys an expected linear relationship with respect to the Hammet parameter σ_p. An important finding of our work is that the excited state pK_a^* also obeys a linear relationship with respect to σ_p. Interestingly, the excited state pK_a^* is ∼5 times more sensitive to the electron-withdrawing power of the substituent than the ground state pK_a. We attribute this difference to the larger polarizability of the excited state charge density. Increase in pK_a due to optical excitation ranging between 2.2 (R = CN) and 10.6 (R = NH_2) units were observed within the set. This substantial range of ΔpK_a values may find use in applications such as oxidation catalysis, in which optically induced removal of protons could speed up reaction kinetics. Finally, we comment on the correlation between photobasicity and enhancement of electronic charge density on the heterocyclic nitrogen upon optical excitation.

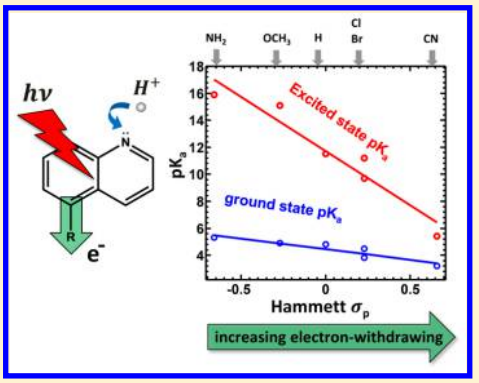

Understanding proton transfer reactions, particularly in the electronic excited state, has received renewed attention in the context of solar-to-fuel light harvesting. The purpose of artificial photosynthesis is to use energy from sunlight to drive redox reactions that convert abundant feedstock to fuels. Such redox reactions often involve both electron and proton transfer, and often with coupled kinetics. It is necessary to understand the mechanism of such reactions and, in particular, to understand how light excitation couples to electronic excitation and eventually to protonic motion.

A well documented case of proton transfer initiated by light occurs in photoacids, which are molecules that become more acidic in their electronically excited state ($pK_a^* < pK_a$).[1−4] In some cases, ΔpK_a can be as large as 12 units.[5] A hydroxyl group attached to a conjugated organic ring such as naphthalene and pyrene is a common moiety in many photoacids. A large body of knowledge exists for photoacids, the prototypical examples being 1-naphthol, 2-naphthol, and 8-hydroxypyrene-1,3,6-trisulfonic acid.[6−11]

The fundamental processes leading to photoacidity have been discussed in the literature. Previous works in this area by Fayer,[12,13] Solntsev,[14,15] Pines,[3] Nibbering,[16] and Hynes[17,18] have considered whether optically induced charge transfer or electronic relaxation in response to proton transfer (i.e., stabilization of the conjugate base) is the main driver of the proton transfer. Later, we will pose and address a similar question for photobases.

Although the molecular physics of photoacids is of interest for investigating fundamentals about hydrogen bonding and proton transfer to solvents,[13,19,20] their transient pH jump[21] capabilities find application in a variety of challenging chemical kinetics problems. For example, they have been used to study protein folding[22] and to elucidate the mechanism of an H_2 evolution catalyst.[23] They have been used as probes of solvent environments on long[10] and transient time scales.[24] Additionally, they have been used in a steady-state manner to control the local pH via light intensity, allowing for the optical regulation of an enzymatic reaction.[25] Recently, a photoacid was used to change the steady state low frequency AC proton conductivity of a material[26] and to mediate an acid catalyzed polymerization reaction.[27]

Photobases are compounds that become more basic in the excited state ($pK_a^* > pK_a$). Despite their potential utility in

Received: April 13, 2016
Accepted: May 19, 2016
Published: May 19, 2016

DOI: 10.1021/acs.jpclett.6b00790
J. Phys. Chem. Lett. 2016, 7, 2093−2099

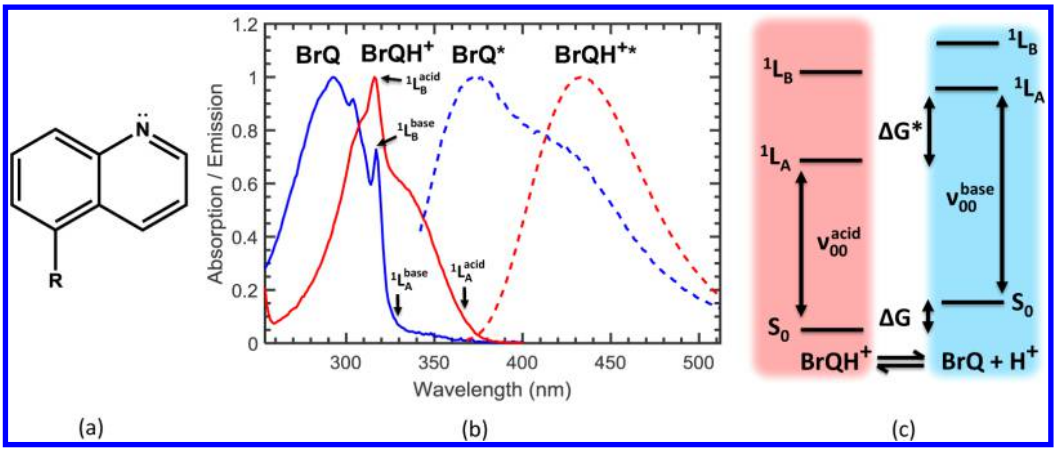

Figure 1. (a) Structure of 5-substituted quinoline. (b) Normalized absorption (solid) and emission (dashed) spectra of 5-bromoquinoline in basic (blue) and acidic (red) aqueous solutions. The approximate origin band energies of the two lowest lying singlet states are annotated. The ^1L_b origin is observed as a sharp feature, whereas the ^1L_a origin is estimated by averaging absorption and emission maxima. For all other compounds in this study, the spectra can be found in the SI. (c) Depiction of the Förster cycle as it applies to quinolines. The excited state equilibrium is between the two lowest lying singlet states.

studying or optimizing chemical reactions requiring pOH jump or assisting the kinetics of reactions that require removal of protons, such as the O_2 evolution half reaction in water splitting ($2\ H_2O \rightarrow O_2 + 4\ H^+ + 4\ e^-$), the available literature on their thermodynamic and kinetic properties is sparse compared to that of photoacids. The common feature in many of the reported photobases is a heterocyclic nitrogen, particularly in a naphthalene framework. Notable examples of photobases are curcumin,[28] xanthone,[29] and 3-styrylpyridine[30] and the phenomenon has been described in a review by Arnaut and Formosinho.[1] Reports of light induced basicity include proton removal from water by 6-aminoquinoline[31] and pOH jump by photoexcitation of acridine[32−34] and 6-methoxyquinoline.[33,35,36] Recently, 6-carboxy-2-naphthol was shown to contain both photoacidic and photobasic functional groups.[37,38]

We were led to this phenomenon by our earlier work on excited state intramolecular proton transfer (ESIPT).[39] We noted that optical excitation appears to redistribute charge within the molecule in such a way that both the acidity of the proton donor and the basicity of the proton acceptor is enhanced. From this, we were led to investigate only the enhanced basicity component of the ESIPT process. The acceptor moiety in our previous study was a nitrogen involved in a conjugated system. Thus, we sought to understand photobasicity in heterocyclic nitrogen containing compounds with the hypothesis that photobasicity in such systems will have similar trends and behavior as their photoacidic counterparts. As just mentioned, we found that such systems were referred to in the earlier literature but were not studied or understood as extensively as the photoacids.

In this work, we investigate the origin and tunability of photobasicity in the 5-substituted quinoline (5-RQ) family of heterocyclic nitrogen-containing compounds, comprising 5-aminoquinoline (AQ), 5-methoxyquinoline (MeOQ), quinoline (Q), 5-bromoquinoline (BrQ), 5-chloroquinoline (ClQ), and 5-cyanoquinoline (CNQ), spanning a large range of electron-withdrawing capability of the R group. This family was chosen so that it can be compared and contrasted to its photoacid counterpart, 5-substituted 1-naphthol, which has been studied before for the effect of substitution on ground and excited state pK_a.[40]

This work aims to answer the following questions: What are the electronic origins of photobasicity? Is the pK_a^* linearly tuned with respect to the Hammett parameter of the substituent? What is different between the sensitivity of the ground and excited state pK_a to the substituent? More generally, can the large knowledge of photoacid systems be extended to structurally similar photobases? Is optically induced charge accumulation on the heterocyclic nitrogen the main contributor to photobasicity? And finally, at what value of the substituent's Hammett parameter is photobasicity extinguished?

We hope that this work will help introduce photobases as modules in the toolkit of synthetic chemists and inspire incorporating them as functional elements in photocatalysts to drive reactions in which removal of protons using light is necessary. Recently, calculations by Hammes-Schiffer's group[41] revealed that it is possible to tune the energetic landscape of the catalytic cycle of a cobalt diglyoxime hydrogen evolution catalyst with the choice of substituents on the ligands. They showed that the reduction potentials of various steps of the catalytic cycle scale linearly with the Hammett parameters of the substituents. We anticipate that tuning the local environment of an oxidation catalyst with photobases and using the excited state pK_a as a means of removing the protons in an oxidation process will prove useful in lowering overpotentials.

We begin with an introduction to the electronic states of quinolines. It is known that two excited electronic states of quinolines are accessible in the UV−visible range of the spectrum. The excited states of quinoline are labeled following the common Platt notation for cata-condensed aromatic systems as ^1L_a and ^1L_b.[42] The ^1L_a state corresponds to atom centered excess charge density compared to the ground state, while the ^1L_b state corresponds to bond centered excess charge density. Thus, creating the ^1L_a state via optical excitation pushes charge density on the heterocyclic nitrogen, and as will be discussed later, is important in making it more basic. Transition to the ^1L_a state corresponds to a broad line shape, whereas excitation to the ^1L_b state results into a sharper absorption line, often with vibronic structures.

The excited state acidity and basicity is commonly inferred from a thermodynamic cycle originally reported by Förster,[43] depicted in Figure 1.c. The approximations and conditions for the validity of the Förster cycle are discussed in several

DOI: 10.1021/acs.jpclett.6b00790
J. Phys. Chem. Lett. 2016, 7, 2093−2099

references.[2,44] In brief, it can be thought of as a thermodynamic cycle involving the protonated and deprotonated forms in both ground and excited states. The ground state pK_a is determined by the difference in energy between the ground state protonated and deprotonated forms as pK_a = $\Delta G/(2.3RT)$. This value is obtained from a conventional titration experiment of the ground state. The next relevant quantity is the 0−0 energy gaps between the ground state and the *lowest* excited electronic states for both the protonated and deprotonated forms. The lowest excited state is chosen because of a general and reasonable assumption in Förster cycle analysis, in which full electronic relaxation within the excited states is completed before proton transfer (i.e., excitation to S_n will rapidly decay such that the excited state acid−base equilibrium is in S_1). This separation of time scales is the basis for using thermodynamic language and concepts such as equilibrium constants for a system in the excited state. The S_0−S_1 gap between 0 and 0 vibrational states can be obtained from the absorption spectrum of the protonated and deprotonated forms alone. However, in practice the vibronic features are poorly distinguishable and it is best to obtain both the absorption and emission spectra for each species and estimate the 0−0 gap as the average between the absorption and emission maxima. Further details of the assignment of the 0−0 gaps for the set of compounds is given in the experimental section. Once the 0−0 transition energies and ΔG are known, the difference in the excited state protonated and deprotonated forms ΔG^* is uniquely defined and is related to the excited state pK_a^* via pK_a^* = $\Delta G^*/(2.3RT)$. As a convenient reference number, an energy gap of 477 cm^{-1} (59 meV) corresponds to one unit of pK_a at T = 298 K. See SI for full derivation.

As a representative spectrum of the 5-substituted quinoline family, the absorption and emission spectra of BrQ in protonated and deprotonated forms are shown in Figure 1b. The spectra for other compounds are shown in the SI. The characteristic sharp ^1L_b states are prominent in the absorption spectrum and do not show frequency shift due to protonation. The broad ^1L_a peak, on the other hand, seems to red shift with protonation. This is consistent with the picture described earlier that optical excitation of the ^1L_a transition creates excess charge density on the atom, in particular the nitrogen heteroatom, thus rendering the corresponding peak more sensitive to protonation. We need to identify the lowest energy 0−0 gap for the Förster cycle analysis. For some compounds, it is necessary to fit the spectra with contributions from the ^1L_a and ^1L_b states and isolate the peak position with the lower energy. As mentioned earlier, the gaps are found by averaging the emission peak and the relevant absorption peak for each species. The results of the Förster cycle analysis are presented in Table 1.

Table 1. Approximate Origin Band Transition Energies, pK_a, and pK_a^* for the Set of 5-R-Quinolines[a]

R	$^1L_a^{base}$	$^1L_b^{base}$	$^1L_a^{acid}$	$^1L_b^{acid}$	ΔpK_a	pK_a	pK_a^*
NH_2	27.0	31.8	21.9	31.8	10.6	5.3	15.9
MeO	28.3	31.9	23.4	31.7	10.2	4.9	15.1
H	31.9	31.9	28.7	31.9	6.7	4.8	11.5
Br	30.4	31.5	27.2	31.6	6.7	4.5	11.2
Cl	30.1	31.5	27.3	31.6	5.9	3.8	9.7
CN	31.8	31.3	30.2	31.3	2.2	3.2	5.4

[a]Energies shown in $cm^{-1} \times 10^3$

Our next goal is to plot the obtained energies and pK_a values as a function of the known electron withdrawing powers of the substituents. In physical organic chemistry there are systematic procedures for quantifying the electron-withdrawing power of a functional group.[45] A commonly used method is called the Hammett analysis. In brief, the acid dissociation constant K_0 of unsubstituted benzoic acid is taken as a reference reaction (pK_a = 4.2). To measure the influence of functional groups R on this value, the acid dissociation constants K of a series of R-substituted benzoic acids are measured. Through a large number of experimental measurements, a simple linear relation $\log \frac{K}{K_0} = \sigma\rho$ is verified, where ρ is a constant and σ is a measure of the electron-withdrawing capability of the functional group. Groups with larger σ pull the electronic charge away from the acidic end of the molecule and thus result into easier dissociation of the proton. We note that several variants of the Hammett parameter exist, some obtained with different reference reactions, some accounting for the position of the substituent on the benzoic acid ring, and some dissecting the inductive and resonance effects in electron withdrawing. We have chosen to use the Hammett parameter σ_p of the studied substituents corresponding to the para-substituted benzoic acid. In practice, correlation with all parameters can be made. We found that σ_p had the best correlation in the ground state, in accordance with prior work,[46] and σ_- had best correlation in the excited state, though all parameters had similarly good correlations. Further information on this is provided in the SI. The trends reported hold true for all parameters, but for the purpose of displaying the information graphically we used σ_p because it had the highest ground state correlation. The values of σ_p used in our work were obtained from ref 47. We point out that the central message of our work does not critically depend on a particular choice of Hammett parameters.

Figure 2 shows the dependence of the energies of various electronic states on the Hammett parameters σ_p of the substituents. To assist comparison of energy gaps for each compound, the $S_0(RQH^+)$ state is set as the reference of energy

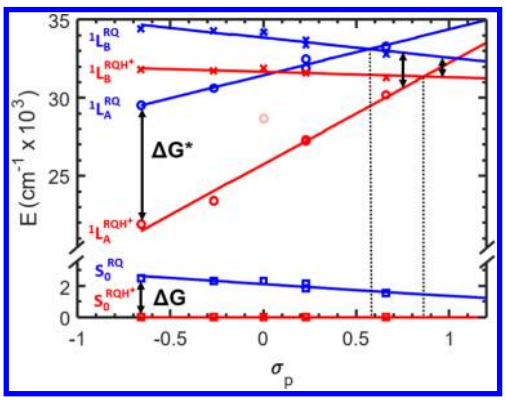

Figure 2. Dependence of ^1L_a and ^1L_b states for protonated and deprotonated forms on the Hammett parameter of the substituents. Straight lines are approximate fits (with the exclusion of unsubstituted quinoline, shown in light red/blue, as described in the text). The lowest excited state is $^1L_A(RQH^+)$ throughout the range of the study. The excited state ΔG^* for protonation is far more favorable than the ground state ΔG, giving rise to photobasicity. Hammett values for which the ^1L_a and ^1L_b states becomes possibly degenerate, are indicated by the vertical dashed line. The difference $\Delta\Delta G = \Delta G^* - \Delta G$, determining ΔpK_a seems to rapidly diminish upon crossing the point of degeneracy of the ^1L_a state for the deprotonated form.

DOI: 10.1021/acs.jpclett.6b00790
J. Phys. Chem. Lett. 2016, 7, 2093−2099

(the lowest red line in the figure). As expected, with increasing Hammett parameter values, the gap ΔG between the $S_0(RQH^+)$ and $S_0(RQ)$ shrinks. Otherwise stated, under equilibrium conditions, larger deprotonated population is expected with larger σ_p, or the acidity of the compound increases with larger σ_p. The ground state pK_a based on this gap is shown in Figure 3. If the dependency is fitted to a straight line, a slope of $\rho = 1.6$ is obtained. This result for the ground state pK_a is reasonably expected and is neither a surprise nor a main point of this study.

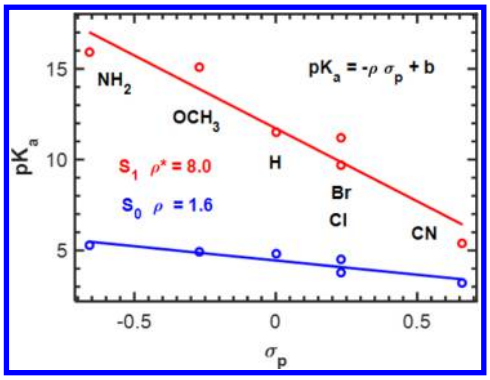

Figure 3. Ground and excited state pK_a of 5-substituted quinolines versus Hammett σ_p parameter. Lines of linear fit are shown in solid. The two central findings of our work are the linear dependence of the excited state pK_a^* on σ_p and its larger slope $\rho^* \sim 5\rho$.

Now, we turn our attention to the excited state protonation gap, in particular for the most negative value of the Hammett parameter $\sigma_p = -0.7$ corresponding to AQ. The most immediate observation is that the excited state gap between the protonated and deprotonated forms is much larger than the ground state. This implies that the protonation of the molecule in the excited state is much more favorable than in the ground state. Translated in pK_a^* form, this information is shown in Figure 3. On the basis of the Förster cycle estimate, upon optical excitation, AQ jumps from a pK_a near 5 to a pK_a^* near 16. This large increase in basicity upon optical excitation is the central point of this work.

Next, we follow the trend in pK_a^* with respect to the Hammett parameter σ_p. A quick observation in Figure 2 shows that the excited state gap ΔG^* becomes smaller as σ_p increases. The $^1L_A(RQH^+)$ state remains the lower state throughout the range of our study $-0.7 < \sigma_p < +0.7$. However, a gentle extrapolation shows that near $\sigma_p \sim 0.9$ the $^1L_A(RQH^+)$ and $^1L_B(RQH^+)$ states must become degenerate. We will comment further on this point later. Similarly, the $^1L_A(RQ)$ and $^1L_B(RQ)$ states become degenerate near $\sigma_p \sim 0.7$. The protonation gap ΔG^* expressed as an excited state pK_a^* is shown in Figure 3. Two central important messages of this work are contained in this figure. The first result is that the excited state pK_a^* follows a linear relation with respect to the Hammett parameter σ_p. The second result is that the slope of this linear relation $\rho^* = 8$ is much larger than the slope of the ground state pK_a. We will explain the possible origin of this difference along with a comparison to the photoacids shortly. This result is similar to the behavior for 5-substituted 1-naphthol,[40] where the excited state has a linear but more sensitive dependence on the Hammett parameter compared to the ground state.

Finally, we list some interesting observations in the series of molecules studied. Some of these observations shed further light on the results presented so far and some may form basis for further studies.

Inspired by the approach and possible crossing of states at high σ_p values (Figure 2), we investigated the spectra of a substituted quinoline with σ_p higher than —CN. An accessible choice for us was R = NO_2 with $\sigma_p = 0.78$. From Figure 2, one infers that, given the line width of transitions, there would not be much distinction between the ^1L_a and ^1L_b states and there would be minimal spectral change upon protonation. Our measured absorption spectrum for the NO_2Q is included in the SI. Indeed, the sharp ^1L_b features, which are present in CNQ, are no longer observed in NO_2Q, and there is minimal red shift upon protonation. For this reason, it is difficult to assign the ground and excited state pK_a values. However, because this behavior is consistent with Figure 2, we plausibly suspect that at this Hammett parameter value the protonated ^1L_a and ^1L_b states are close to degeneracy. Furthermore, it is inferred that for NO_2Q the drive for protonation in the excited state ΔG^* is not very different from ΔG. Thus, this work not only reports a trend for photobasicity but also predicts that photobasicity can be turned off for a value of $\sigma_p \sim 0.8$ due a substituent R = NO_2.

Because Hammett parameters are not inferred from measurement of spectroscopic gaps, it is not immediately obvious that one should expect the linear relationship in Figure 2. Otherwise stated, the Hammett analysis is not related to or based upon optical spectroscopy data but rather demonstrates a trend in ground state thermodynamic drives. The Förster cycle is built to relate spectroscopic gaps to thermodynamics drives in the ground and excited states. Thus, Hammett parameters are indirectly and subtly related to spectroscopic gaps via the Förster cycle.

A notable break in the trends shown in Figure 2 is quinoline itself. The behavior of its states with respect to protonation is the same as the other compounds in that its ^1L_b is invariant to protonation and ^1L_a red shifts upon protonation. However, the energies of these transitions are significantly higher than the energies of the corresponding transitions in neighboring MeOQ and BrQ. For this reason, they have been excluded from the fits shown in Figure 2. Despite this apparent anomaly the pK_a^* value calculated with the Förster cycle for quinoline does lay in the same line as the other compounds. These observations may seem odd at first, but in fact the perceived oddity is clarified once we consider the origin of the Hammett parameters, which were meant to correlate *ground state* equilibria to a reference reaction with a resulting linear relationship as pointed out in the previous paragraph. We suspect that the spectroscopic gaps of unsubstituted quinoline (R = H) are an exception to the correlations in Figure 2 because of the small size of the hydrogen atom. Its ability to modulate excited states by pushing and pulling electrons is captured, or rather defined, with its Hammett parameter $\sigma_p = 0$. What is not captured in σ_p is how R extends the size of the π system. The other substituents are fairly large with respect to hydrogen and are larger perturbations to the particle on a ring model of the molecule. Even if they do not participate in the conjugation, they serve as partial extenders of electron density, thus lowering the transition energies to the first excited state. For R = H, the π system is less delocalized and consequently the ^1L_a and ^1L_b energies are larger compared to its neighboring compounds, as seen in Figure 2. As an argument in favor of this proposal, in the TD-DFT exitation energies and electron density difference maps, we do see that even though the ^1L_a

DOI: 10.1021/acs.jpclett.6b00790
J. Phys. Chem. Lett. 2016, 7, 2093−2099

excitation is primarily HOMO to LUMO (π to π^*), electron density changes do occur on the substituent (Figure S2).

Previous work on intramolecular charge transfer (ICT) in neutral photoacids (hydroxypyrene derivatives,[12,16] naphthol derivatives,[17,48] and phenol derivatives[18,49]) has shown that ICT on the conjugate photobase is typically larger than ICT on the photoacid, although the reverse situation is true in the cationic photoacid APTS.[13] Mulliken charge density analysis on the quinoline derivatives studied has found approximately equal ICT on the photobase and conjugate photoacid upon optical excitation (Figure S1), suggesting that they may be different than traditional photoacids. We invite theoreticians to investigate the phenomenon more thoroughly with advanced charge analysis methods.

We have not included any potential contribution from triplet states or the rates of intersystem crossing or nonradiative decay. While it is possible that a T_1 acid−base equilibrium also exists, it does not preclude the pK_a^* values discussed above. Previous work has shown that in solvated quinoline at low temperatures fluorescence originates only from hydrogen bonded species, while phosphorescence arises from non-hydrogen bonded species.[50] Additionally they, and others,[51] have pointed out that the broad, dual emission observed is from an excited state proton transfer.

In conclusion, we have measured the magnitude and tunability of photobasicity in 5-substituted quinolines. The pK_a and pK_a^* in the studied set of compounds correlate to Hammett σ_p parameter over the chemical space investigated ($-0.7 < \sigma_p < 0.7$). The 0−0 energies of the states themselves, with the exception of unsubstituted quinoline, also obey a linear relation with respect to σ_p. The relative energies of the ^1L_a states of the acid and base forms are responsible for the ΔpK_a values, with the exception of the larger electron withdrawing region ($\sigma_p > 0.55$). Synthetic efforts to increase ΔpK_a or select a desired pK_a^* value should focus on the relative interaction of the substituent with the ^1L_a states. We envision that this quantitative measurement of the substituent effect on the ground and excited state equilibria will allow one to carefully select the desired ΔpK_a for an application requiring removal of protons, for example in an oxidation catalyst.

EXPERIMENTAL SECTION

A set of six compounds in aqueous solution had their absorption and emission spectra measured: 5-aminoquinoline (AQ), 5-methoxyquinoline (MeOQ), quinoline (Q), 5-bromoquinoline (BrQ), 5-chloroquinoline (ClQ), and 5-cyanoquinoline (CNQ). The absorption of 5-nitroquinoline (NO_2Q) was also analyzed. AQ, MeOQ, BrQ, and CNQ were purchased from Combi-Blocks. Q, ClQ, ad NO_2Q were purchased from Sigma-Aldrich. All compounds were used without further purification.

Absorption spectra were obtained using a Cary 50 UV−vis spectrophotometer. Emission spectra were collected on a Jobin-Yvon Fluoromax 3 fluorimeter. Addition of HCl or NaOH to aqeuous solutions of each compound were made to titrate the pH which was measured with a Hanna Instruments HI 2210 pH meter. The procedure reported by Schrager[52] was used to calculate the pK_a from spectroscopic data. Briefly, singular value decomposition was used to find the variation of quinoline/quinolinium population with pH. This variation was fitted to the Henderson-Hasselbach equation to determine the pK_a.

In using the Förster cycle to calculate pK_a^*, the 0−0 transition energies of the acid and base forms need to be identified.[44] The sharp ^1L_b vibronic progressions were observed from UV−vis absorption spectra for all compounds except the deprotonated form of AQ. The longest wavelength peak in the progression was taken as the ^1L_b 0−0 transition.[51] Fluorescence spectra were collected to identify each species' emission maxima. As reported before, the absorption and emission maxima for a given species were averaged as a means to estimate the ^1L_a 0−0 transition for both protonated and deprotonated forms.[2] In the cases where the ^1L_a and ^1L_b absorption bands were overlapping, numerical values for the peak positions were obtained by fitting the spectra with Gaussians. Details on estimation of pK_a^* based on this data is presented in the discussion section.

The emission of the neutral MeOQ and Q species were weak compared to their cations. In these cases, the emission in methanol was used to identify the peak of the neutral species. This energy was corrected by subtracting the solvatochromatic shift observed for the cation peak in water and methanol solutions. All absorption and emission spectra and fits for each compound are available in the SI.

Computational Methods. Electron density difference maps and Mulliken charges were computed using the Q-Chem[53] software package and plotted with VMD.[54] Ground state geometries were optimized with B3LYP/6-31+G*. Excited state electron densities and Mulliken charges were calculated using TD-DFT/B3LYP/6-31+G* and plotted at the $\pm$0.0005 isosurfaces.

ASSOCIATED CONTENT

Supporting Information

The Supporting Information is available free of charge on the ACS Publications website at DOI: 10.1021/acs.jpclett.6b00790.

A collection of absorption and emission spectra for the set of compounds studied is supplied. (PDF)

AUTHOR INFORMATION

Corresponding Author

*E-mail: dawlaty@usc.edu. Tel.: 213-740-9337.

Notes

The authors declare no competing financial interest.

ACKNOWLEDGMENTS

The authors acknowledge support from the University of Southern California start up grant and the AFOSR YIP Award (FA9550-13-1-0128).

REFERENCES

(1) Arnaut, L. G.; Formosinho, S. J. Excited-state proton transfer reactions I. Fundamentals and intermolecular reactions. *J. Photochem. Photobiol., A* **1993**, *75*, 1−20.

(2) Ireland, J. F.; Wyatt, P. A. H. Acid-Base Properties of Electronically Excited States of Organic Molecules. *Adv. Phys. Org. Chem.* **1976**, *12*, 131−221.

(3) Pines, D.; Nibbering, E. T. J.; Pines, E. Monitoring the Microscopic Molecular Mechanisms of Proton Transfer in Acid-base Reactions in Aqueous Solutions. *Isr. J. Chem.* **2015**, *55*, 1240−1251.

(4) Solntsev, K. M.; Sullivan, E. N.; Tolbert, L. M.; Ashkenazi, S.; Leiderman, P.; Huppert, D. Excited-state proton transfer reactions of 10-hydroxycamptothecin. *J. Am. Chem. Soc.* **2004**, *126*, 12701−12708.

(5) Simkovitch, R.; Karton-Lifshin, N.; Shomer, S.; Shabat, D.; Huppert, D. Ultrafast excited-state proton transfer to the solvent occurs on a hundred-femtosecond time-scale. *J. Phys. Chem. A* **2013**, *117*, 3405−3413.

DOI: 10.1021/acs.jpclett.6b00790
J. Phys. Chem. Lett. 2016, 7, 2093−2099

(6) Tolbert, L. M.; Solntsev, K. M. Excited-State Proton Transfer: From Constrained Systems to "Super" Photoacids to Superfast Proton Transfer. *Acc. Chem. Res.* **2002**, *35*, 19−27.
(7) Agmon, N. Primary events in photoacid dissociation. *J. Mol. Liq.* **2000**, *85*, 87−96.
(8) Agmon, N. Elementary Steps in Excited-State Proton Transfer. *J. Phys. Chem. A* **2005**, *109*, 13−35.
(9) Messina, F.; Prémont-Schwarz, M.; Braem, O.; Xiao, D.; Batista, V. S.; Nibbering, E. T. J.; Chergui, M. Ultrafast solvent-assisted electronic level crossing in 1-naphthol. *Angew. Chem., Int. Ed.* **2013**, *52*, 6871−6875.
(10) Barrash-Shiftan, N.; Brauer, B.; Pines, E. Solvent dependence of pyranine fluorescence and UV-visible absorption spectra. *J. Phys. Org. Chem.* **1998**, *11*, 743−750.
(11) Spies, C.; Shomer, S.; Finkler, B.; Pines, D.; Pines, E.; Jung, G.; Huppert, D. Solvent dependence of excited-state proton transfer from pyranine-derived photoacids. *Phys. Chem. Chem. Phys.* **2014**, *16*, 9104−14.
(12) Silverman, L. N.; Spry, D. B.; Boxer, S. G.; Fayer, M. D. Charge transfer in photoacids observed by stark spectroscopy. *J. Phys. Chem. A* **2008**, *112*, 10244−10249.
(13) Spry, D. B.; Fayer, M. D. Charge redistribution and photoacidity: Neutral versus cationic photoacids. *J. Chem. Phys.* **2008**, *128*, 084508.
(14) Solntsev, K. M.; Huppert, D.; Tolbert, L. M.; Agmon, N. Solvatochromic Shifts of "Super" Photoacids. *J. Am. Chem. Soc.* **1998**, *120*, 7981−7982.
(15) Solntsev, K. M.; Huppert, D.; Agmon, N. Solvatochromism of β-Naphthol. *J. Phys. Chem. A* **1998**, *102*, 9599−9606.
(16) Mohammed, O. F.; Dreyer, J.; Magnes, B. Z.; Pines, E.; Nibbering, E. T. J. Solvent-dependent photoacidity state of pyranine monitored by transient mid-infrared spectroscopy. *ChemPhysChem* **2005**, *6*, 625−636.
(17) Tran-Thi, T. H.; Prayer, C.; Millié, P.; Uznanski, P.; Hynes, J. T. Substituent and solvent effects on the nature of the transitions of pyrenol and pyranine. Identification of an intermediate in the excited-state proton-transfer reaction. *J. Phys. Chem. A* **2002**, *106*, 2244−2255.
(18) Granucci, G.; Hynes, J. T.; Millié, P.; Tran-Thi, T. H. A theoretical investigation of excited-state acidity of phenol and cyanophenols. *J. Am. Chem. Soc.* **2000**, *122*, 12243−12253.
(19) Simkovitch, R.; Akulov, K.; Shomer, S.; Roth, M. E.; Shabat, D.; Schwartz, T.; Huppert, D. Comprehensive study of ultrafast excited-state proton transfer in water and D2O providing the missing RO(−)···H(+) ion-pair fingerprint. *J. Phys. Chem. A* **2014**, *118*, 4425−43.
(20) Simkovitch, R.; Shomer, S.; Gepshtein, R.; Huppert, D. How fast can a proton-transfer reaction be beyond the solvent-control limit? *J. Phys. Chem. B* **2015**, *119*, 2253−2262.
(21) Pines, E.; Huppert, D. pH Jump: A Relaxational Approach. *J. Phys. Chem.* **1983**, *87*, 4471−4478.
(22) Abbruzzetti, S.; Crema, E.; Masino, L.; Vecli, A.; Viappiani, C.; Small, J. R.; Libertini, L. J.; Small, E. W. Fast events in protein folding: structural volume changes accompanying the early events in the N− > I transition of apomyoglobin induced by ultrafast pH jump. *Biophys. J.* **2000**, *78*, 405−415.
(23) Dempsey, J. L.; Winkler, J. R.; Gray, H. B. Mechanism of H2 Evolution from a Photogenerated Hydridocobaloxime. *J. Am. Chem. Soc.* **2010**, *132*, 16774−16776.
(24) Psciuk, B. T.; Prémont-Schwarz, M.; Koeppe, B.; Keinan, S.; Xiao, D.; Nibbering, E. T. J.; Batista, V. S. Correlating photoacidity to hydrogen-bond structure by using the local O-H stretching probe in hydrogen-bonded complexes of aromatic alcohols. *J. Phys. Chem. A* **2015**, *119*, 4800−4812.
(25) Peretz-Soroka, H.; Pevzner, A.; Davidi, G.; Naddaka, V.; Kwiat, M.; Huppert, D.; Patolsky, F. Manipulating and Monitoring On-Surface Biological Reactions by Light-Triggered Local pH Alterations. *Nano Lett.* **2015**, *15*, 4758−4768.
(26) Haghighat, S.; Ostresh, S.; Dawlaty, J. M. Controlling Proton Conductivity with Light: A Scheme Based on Photoacid Doping of Materials. *J. Phys. Chem. B* **2016**, *120*, 1002−07.
(27) Fu, C.; Xu, J.; Boyer, C. Photoacid-mediated Ring Opening Polymerization Driven by Visible Light. *Chem. Commun.* **2016**, DOI: 10.1039/C6CC03084J.
(28) Akulov, K.; Simkovitch, R.; Erez, Y.; Gepshtein, R.; Schwartz, T.; Huppert, D. Acid effect on photobase properties of curcumin. *J. Phys. Chem. A* **2014**, *118*, 2470−2479.
(29) Vogt, S.; Schulman, S. G. Reversible Proton Transfer in Photoexcited Xanthone. *Chem. Phys. Lett.* **1983**, *97*, 450−3.
(30) Favaro, G.; Mazzucato, U.; Masetti, F. Excited state reactivity of aza aromatics. I. Basicity of 3-styrylpyridines in the first excited singlet state. *J. Phys. Chem.* **1973**, *77*, 601−604.
(31) Munitz, N.; Avital, Y.; Pines, D.; Nibbering, E. T. J.; Pines, E. Cation-Enhanced Deprotonation of Water by a Strong Photobase. *Isr. J. Chem.* **2009**, *49*, 261−272.
(32) Nachliel, E.; Ophir, Z.; Gutman, M. Kinetic Analysis of Fast Alkalinization Transient by Photoexcited Hetercyclic Compounds: pOH Jump. *J. Am. Chem. Soc.* **1987**, *109*, 1342−1345.
(33) Pines, E.; Huppert, D.; Gutman, M.; Nachliel, N.; Fishman, M. The pOH Jump: Determination of Deprotonation Rates of Water by 6-Methoxyquinoline and Acridine. *J. Phys. Chem.* **1986**, *90*, 6366−6370.
(34) Liu, X.; Karsili, T. N. V.; Sobolewski, A. L.; Domcke, W. Photocatalytic Water Splitting with the Acridine Chromophore: A Computational Study. *J. Phys. Chem. B* **2015**, *119*, 10664−10672.
(35) Poizat, O.; Bardez, E.; Buntinx, G.; Alain, V. Picosecond Dynamics of the Photoexcited 6-Methoxyquinoline and 6-Hydroxyquinoline Molecules in Solution. *J. Phys. Chem. A* **2004**, *108*, 1873−1880.
(36) Naik, L. R.; Suresh Kumar, H. M.; Inamdar, S. R.; Math, N. N. Steady-State and Time-Resolved Emission Studies of 6-Methoxy Quinoline. *Spectrosc. Lett.* **2005**, *38*, 645−659.
(37) Ditkovich, J.; Mukra, T.; Pines, D.; Huppert, D.; Pines, E. Bifunctional photoacids: Remote protonation affecting chemical reactivity. *J. Phys. Chem. B* **2015**, *119*, 2690−2701.
(38) Ditkovich, J.; Pines, D.; Pines, E. Controlling reactivity by remote protonation of a basic side group in a bifunctional photoacid. *Phys. Chem. Chem. Phys.* **2016**, DOI: 10.1039/C5CP07672B.
(39) Driscoll, E.; Sorenson, S.; Dawlaty, J. M. Ultrafast Intramolecular Electron and Proton Transfer in Bis(imino)isoindole Derivatives. *J. Phys. Chem. A* **2015**, *119*, 5618−5625.
(40) Premont-Schwarz, M.; Barak, T.; Pines, D.; Nibbering, E. T. J.; Pines, E. Ultrafast Excited-State Proton-Transfer Reaction of 1-Naphthol-3,6-Disulfonate and Several 5-Substituted 1-Naphthol Derivatives. *J. Phys. Chem. B* **2013**, *117*, 4594−4603.
(41) Solis, B. H.; Hammes-Schiffer, S. Substituent effects on cobalt diglyoxime catalysts for hydrogen evolution. *J. Am. Chem. Soc.* **2011**, *133*, 19036−9.
(42) Platt, J. R. Classification of Spectra of Cata-Condensed Hydrocarbons. *J. Chem. Phys.* **1949**, *17*, 484.
(43) Förster, T. Elektrolytische Dissoziation angeregter Moleküle. *Zeitschrift für Elektrochemie und angewandte physikalische Chemie* **1950**, *54*, 42−46.
(44) Weller, A. Fast Reactions of Excited Molecules. *Progress in Reaction Kinetics and Mechanism* **1961**, *1*, 187−214.
(45) Anslyn, E.; Dougherty, D. *Modern Physical Organic Chemistry*; University Science: Dulles, VA, 2006.
(46) Charton, M. The Application of the Hammett Equation to Polycyclic Aromatic Sets. I. Quinolines and Isoquinolines. *J. Org. Chem.* **1965**, *30*, 3341−3345.
(47) Hansch, C.; Leo, a.; Taft, R. W. A Survey of Hammett Substituent Constants and Resonance and Field Parameters. *Chem. Rev.* **1991**, *91*, 165−195.
(48) Agmon, N.; Rettig, W.; Groth, C. Electronic Determinants of Photoacidity in Cyanonaphthols. *J. Am. Chem. Soc.* **2002**, *124*, 1089−1096.

DOI: 10.1021/acs.jpclett.6b00790
J. Phys. Chem. Lett. 2016, 7, 2093−2099

(49) Hynes, J. T.; Tran-Thi, T.-H.; Granucci, G. Intermolecular photochemical proton transfer in solution: new insights and perspectives. *J. Photochem. Photobiol., A* **2002**, *154*, 3−11.
(50) Anton, M. F.; Moomaw, W. R. Luminescence and hydrogen bonding in quinoline and isoquinoline. *J. Chem. Phys.* **1977**, *66*, 1808−1818.
(51) Schulman, S. G.; Capomacchia, A. C. Dual Fluorescence of the Quinolinium Cation. *J. Am. Chem. Soc.* **1973**, *95*, 2763−2766.
(52) Shrager, R. I.; Hendler, R. W. Titration of Individual Components in a Mixture with Resolution of Difference Spectra, pKs, and Redox Transitions. *Anal. Chem.* **1982**, *54*, 1147−1152.
(53) Shao, Y.; et al. Advances in molecular quantum chemistry contained in the Q-Chem 4 program package. *Mol. Phys.* **2015**, *113*, 184−215.
(54) Humphrey, W.; Dalke, A.; Schulten, K. VMD - Visual Molecular Dynamics. *J. Mol. Graphics* **1996**, *14*, 33−38.

DOI: 10.1021/acs.jpclett.6b00790
J. Phys. Chem. Lett. 2016, 7, 2093−2099